PHASE VARIATION IN DOPPLER SIGNAL FOR VARIOUS OPTICAL PARAMETERS

Jung-Young Son*, Myung-Sik Kim and Myung-Hwan Oh

Korea Institute of Science and Technology Seoul, Korea

ABSTRACT

The scattered light intensity from a spherical particle passing through the cross-over region of two coherent laser beams, varies periodically. Photodetection of this light beams produces a periodic signal of varying amplitude. The phase of the signal varies with the particle size and refractive index, the beam crossing angle and wavelength, and the position and size of the scattered ligth collecting aperture. In this paper the phase variation with respect to the particle absorptive index of retraction, collecting lens size and beam crossing angle is calculated using both Mie scattering theory and reflection theory. The two theories show good agreement in phase predictions, especially for large absorptive indices and for small collection lenses. Both theories predict phase to be inversely proportional to the beam crossing angle.

INTRODUCTION

Photodetection of the scattered light from a particle moving across the cross-over region of two coherent laser beams, generates two different signals called the Doppler and pedestal signals[1]. The pedestal signal represents the Gaussian beam intensity profile along the particle trajectory in the cross-over region. The pedestal is modulated by the high frequency Doppler signal. The period of the Doppler signal is a function of the particle speed, beam crossing angle and the wavelength of the laser beams. For a given beam crossing angle, beam wavelength, beam polarization direction relative to its propergation direction, and collecting lens size and location relative to the cross-over region, the phase of the Doppler signal relative to the pedestal signal comprises information about particle characteristics including size, refractive index and shape[2].

For large spherical particles, the diffraction lobe is confined to a very narrow region about the incident beam direction. Then, the phase of light scattered to a point in space is determined by the path length difference between the reference ray and refracted rays, and between different refracted and reflected rays from the particle. When a particle is absorptive, the refracted ray contribution is negligible, and phase is solely determined by the path difference between the reflected rays of beams 1 and 2.

The characteristics of Doppler signal phase have been evaluated or "calibrated" by several authors using either Mie scattering theory or geometrical optics theory[2-5].

However, no comparison between the generalized Mie scattering solution[6] and a geometrical optics approximation has been made. In this paper, variations in the phase of the Doppler signal, relative to the pedestal signal, are analyzed over the particle diameter range 0.1 to 18μm.

Both a geometrical optics approximation and the generalized Mie scattering solution are used with a 0.1 μm diameter interval, looking at the variations for several refractive indices, incident beam crossing angles, and collecting lens sizes.

PHASE ANGLE

In the dual cross-beam geometry, the scattered light energy, I, on the surface of a collecting aperture in an arbitrary location is expressed as[7] ;

$$I = \frac{1}{2}\mathrm{Re}[I_{11} + I_{22} + I_{12}\exp(i\omega_d t) + I_{21}\exp(-i\omega_d t)], \quad (1)$$

where scattered energy from beams 1 and 2 and beam interference is expressed as I_{11}, I_{22}, I_{12} and I_{21}, and ω_d is the angular Doppler frequency due to motion of the particle relative to the propagating beams, Equation (1) can be rewritten as

$$I = I_{dc} + I_{ac}\cos(\omega_d t + \phi), \quad (2)$$

where I_{dc} is $\mathrm{Re}(I_{11} + I_{22})/2$, I_{ac} is,

$$I_{ac} = \{[\mathrm{Re}(I_{12} + I_{21})]^2 + [\mathrm{Im}(I_{21} - I_{12})]^2\}^{1/2}, \quad (3)$$

and the Doppler phase angle is,

$$\phi = \tan^{-1}\left\{\frac{\mathrm{Im}(I_{21} - I_{12})}{\mathrm{Re}(I_{21} + I_{12})}\right\} \quad (4)$$

As shown in Equation (4), ϕ is a function only of scattered light energy terms I_{12} and I_{21}. Thus, ϕ is a function only of particle characteristics (including size, reflective index and shape) and optical parameters (including beam crossing angle, beam polarization direction and collecting lens size and location). In geometrical optics the incident, reflected and transmitted rays are all in the beam incidence plane. When a plane wave is incident on the surface of a spherical particle, the beam incidence plane contains a cross-section of the particle. Since rays in a beam have the same propagation direction as the beam, the rays in one beam reflected at the surface of the particle will not intersect. Rays from beams of different propagation direction will intersect. If the amplitude of Doppler shifted rays from each incidence beam is represented as $E_1\exp(\omega_1 - \bar{k}\cdot\bar{R}_1 + \phi_1)$ and $E_2\exp(\omega_2 - \bar{k}\cdot\bar{R}_2 + \phi_2)$, respectively. Where ω_1 and ω_2 are Doppler shifted angular frequency of the reflected rays, k is propagation constant in the direction of a intersecting point of the reflected rays, $\bar{R}_1$ and $\bar{R}_2$ are direction vector of the reflected rays, and ϕ_1 and ϕ_2 are initial phase of the reflected rays from beams 1 and 2, respectively. $\omega_1 - \omega_2$ gives Doppler frequency of the resulted signal and the phase difference of the Doppler signal is given as $\bar{k}\cdot(\bar{R}_1 - \bar{R}_2) + (\phi_1 - \phi_2)$. Figure 1 shows the scattering geometry of rays of beams 1 and 2 reflected at the surface of a spherical particle. In this figure, it is assumed that the particle is at point O, the center of the spherical coordinates. Considering a particle cross-section plane for specific rays in each beam, select a reflected ray from each beam, which meets at point C at (r, θ, ψ) on the intersection line of the two beam incidence planes. As shown in figure 1, $\bar{k}\cdot(\bar{R}_1 - \bar{R}_2) + (\phi_1 - \phi_2)$ for small values of α_1 and α_2 is given as $(2\pi/\lambda)\{(R_1' - R_2) + (R_1' - R_2)\}$, i.e., the phase difference of the Doppler signal is propotional to the path length difference between reflected rays, $(R_1' + R_1) - (R_2' + R_2)$. for small values of α_1 and α_2. R_1 and R_1 are expressed as,

$$R_1' = a(1 - \cos\gamma_1), \tag{5}$$

$$R_1 = [r^2 + a^2 + 2ra\cos\{180^\circ - (\gamma_1 + \theta_1)\}]^{1/2}$$

$$\simeq r\{1 + \frac{a}{r}\cos(\theta_1 + \gamma_1)\}, \tag{6}$$

where a is the particle radius, R_2' and R_2 are expressed by Equations (5) and (6) with subscript 1 changed to subscript 2. In figure 1 triangle OPC for ray 1 has the angles COP and CPO defined as $180^\circ - \gamma_1$, respectively. Since $r >> a$, $\alpha_1 \simeq 0$ and $\gamma_1 = 90^\circ - \theta_1/2$. Similary $\alpha_2 \simeq 0$ and $\gamma_2 = 90^\circ - \theta_2/2$. Substituting γ_1 into Equations (5) and (6),

$$R_1' = a\{1 - \sin(\theta_1/2)\} \tag{7}$$

and

$$R_1 = r - a\sin(\theta_1/2) \tag{8}$$

Hence,

$$(R_1' + R_1) - (R_2' + R_2) = 2a\{\sin(\theta_2/2) - \sin(\theta_1/2)\}. \tag{9}$$

From the spherical harmonics addition theorem, θ_1 is given as,

$$\cos\theta_1 = \sin\theta\sin\phi\sin(\xi/2) + \cos\theta\cos(\xi/2)$$

$$= A\cos(\xi/2 - \beta). \tag{10}$$

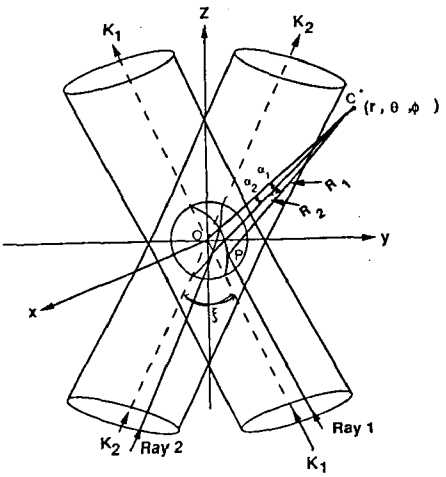

a) Particle in Crossed Beams

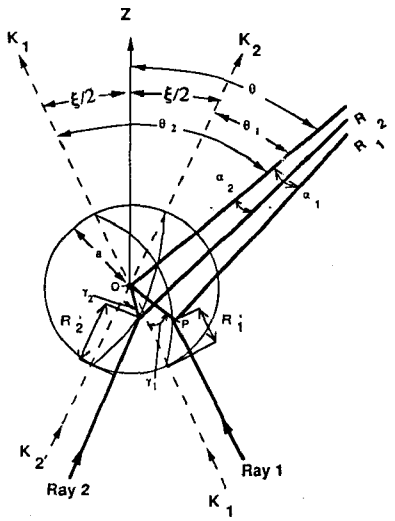

b) Rays Scattered from Particle Surface

Figure 1. Scattering Geometry

Where $A = (\cos^2\theta + \sin^2\theta\sin^2\phi)^{1/2}$ and $\beta = \tan^{-1}(\sin\theta\sin\phi/\cos\theta)$. Replacing ξ with $-\xi$ in Equation (10) gives the expression for $\cos\theta_2$. Since $\sin(\theta/2) = \{(1 - \cos\theta)/2\}^{1/2}$, Equation (9) can be rewritten as,

$$(R_1' + R_1) - (R_2' + R_2)$$
$$= 2^{1/2}a[\{1 - A\sin(\xi/2 - \beta)\}^{1/2} - \{1 - A\sin(\xi/2 + \beta)\}^{1/2}]$$
$$\simeq \frac{Aa}{\sqrt{2}}\{\cos(\xi/2 + \beta) - \cos(\xi/2 - \beta)\}$$
$$= -2^{1/2}Aa\sin(\xi/2)\sin\beta. \qquad (11)$$

The phase angle difference between two reflected rays is given as,

$$\phi = -\frac{2\pi}{\lambda}\sqrt{2}Aa\sin(\xi/2)\sin\beta$$
$$= -\frac{1}{\sqrt{2}\delta}\pi DA\sin\beta, \qquad (12)$$

where D is particle diameter and $\delta = \lambda/2\sin(\xi/2)$ is called the fringe period.[8]

Equation (12) shows the phase angle difference between reflected rays from beams 1 and 2 is linearly proportional to the particle diameter and position of the collecting aperture, and is inversely proportional to the fringe period. Furthermore, this phase angle difference is dependent only to the direction of the intersection point of the reflected rays. This means that the phase angle of the Doppler signal is independent to the size of light collecting aperture. For the derivation of Equations (5) - (7), no contribution from the internally reflected rays was considered. When particles have high absorptive index, the effects of the internally reflected rays will be minimal. The phase angle difference will be independent to the particle refractive index. The results of phase angle computations using both Equations (4), for any particle, and (9), for solely reflective particles, are given in the following section.

COMPUTATIONAL RESULTS

For the computations : 1) The center of the collecting lens is located at a point (r, 54.6°, 29.8°). 2) The distance r is normalized by the lens f/#s of 2, 4, 6 and 8 were considered. 3) The incident laser beam λ is 0.5145μm. 4) The incident beam crossing angles, ξ, are normalized by δ and values of 1, 2, 2.5 and 4μm were considered for δ.

Figure 2 shows phase angle variations with particle refrative index, m = 1.56 - iX, where X, the absorptive index, has values 0.0, 0.01, 0.05, 0.2 and 0.47. Figure 2 Mie theory predictions are for δ = 2.5 μm and f/# = 4. Figure 2 is drawn between equivalent values -180.0^0 and $+180.0^0$; as the phase angle passes through these values it is plotted as a fictitious jump across 0° to indicate continuity. For small size parameters phase has a negative

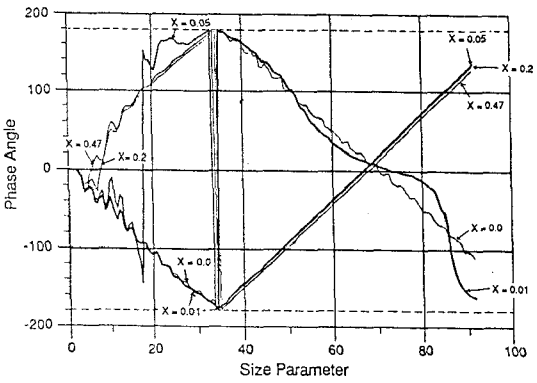

Figure 2. Variation of Phase for Various Absorptive Particles.

polarity, but changes polarity as size parameter increases for $X \geq 0.05$. Except for $X \leq 0.01$, large swings in the phase curves only occur near the polarity change, and the large swings in the X = 0.01 phase curve indicate a sudden polarity change will occur at a size parameter value greater than the maximum computed value of 92. As X increases the phase polarity change occurs at smaller size parameters. After the polarity change the phase variation with size parameter tends toward a linear relationship ; however, the increment in this relationship becomes slight smaller as X increases.

Figure 3 shows phase variations with different combinations δ and f/# for the particle diameter range 0.1 - 18 μm and m = 1.4 - i0. Like figure 2, figure 3 is drawn between equivalent values -180.0^o and $+180.0^o$. For δ = 1 μm and f/# = 2 a phase angle increment of 360^0 corresponds to a size parameter increment of about 26, but then the phase variation with size parameter becomes irregular. Phase variations with size parameter for δ = 1 μm and f/# 2, 4 and 6 are nearly the same until the f/# 2 variation becomes irregular. The f/# 4 and 6 variations remain similar with a 360^0 phase increment for every size parameter increase of 26, until the f/# 4 variation becomes irregular at about a size parameter of about 80. After the variations become irregular, a 360^0 phase increment still occurs at regular size parameter intervals, but the associated intervals are less than 26. The initial size parameter interval associated with a 360^0 phase increment is about 53 for δ = 2 μm and about 106 for δ = 4 μm. The associated size parameter intervals for X = 0.01 are the same as for X = 0.0, but large swings occur in the phase curves at larger size parameter values, similar to the swings noted in figure 2. In summary, figure 3 confirms that: phase increases linearly in proportion to the inverse of the fringe period; a regular variation of phase extends to larger particle sizes as the f/# increases (i.e., phase linearity improves when smaller size collecting lenses are used); and phase becomes less linear with particle size as the particle size increases.

Figure 4 compares phase predictions using Equations (4) and (9) for f/# of 6 vs. 8, and for several refractive indices, m = n - i0.5, with n values of 1.37, 1.56 and 1.77.

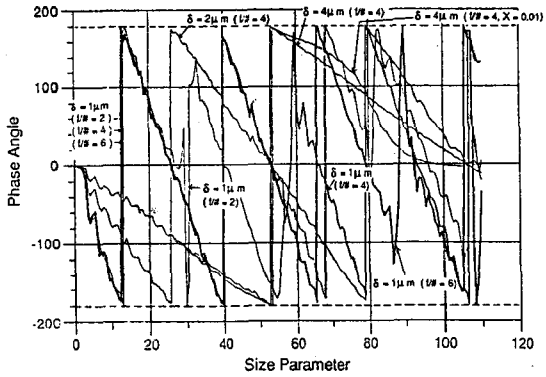

Figure 3. Fringe Period Effects on Scattering Characteristics.

These values correspond to the most common particle refractive indices in coal combustion. As shown in figure 4, the phase increment increases with increasing n, and the smallest increment occurs for n = 1.37, f/# 8. The phase angle predicted by reflection theory is slightly less than for Mie theory with n = 1.37, f/# 6; however it is slightly greater than for Mie theory with n = 1.37, f/# 8. For size parameter values greater than 30 the phase angles with n = 1.77, f/# 6 are within 6^{o} of the angles with n = 1.37, f/# 8. A 6^{0} change in phase corresponds to a size parameter change of about 1.5. This indicates that reflection theory predition of phase variation for large particles is as accurate as Mie theory prediction, and the phase variation is almost indifferent to the particle refractive index. Ocillations in the Mie generated phase curves increase in amplitude as the size parameter value decreases. This indicates that smaller particles are still transparent even when the particle absorptive index of refraction is high, and refracted and diffracted rays affect the phase. When the phase angle difference for the selected intersecting points on surface of light collecting aperture were averaged, the averaged value was slightly less than the phase angle value at the center of the aperture.

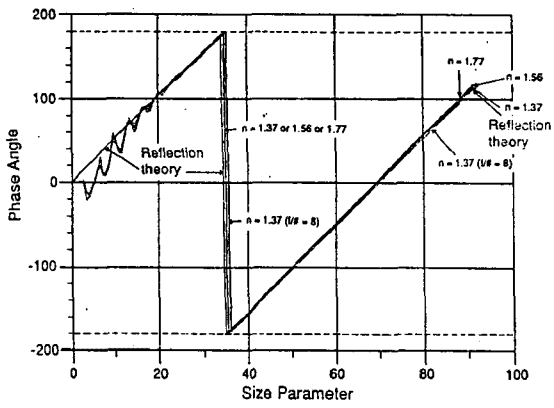

Figure 4. Comparison Between Mie Theory and Reflection Theory for Various Absorptive Particles

CONCLUSION

Reflection theory prediction of relationships between the incident beam crossing angle and phase is accurate even for transparent particle when smaller collecting lenses are used. For highly absorptive particles, the phase variation is well predicted by the reflection theory as long as the size parameter values are greater than 30.

REFERENCE

1. W. M. Farmer, "Measurement of Particle Size, Number density, and Velocity using a Laser Interferometer.", Applied Optics Vol. 11, 2603, 1972.

2. J. Y. Son and T. V. Giel, Jr., "Analysis of Doppler Signal Phase.", Ninth International Conference on Lasers'86, STS Press, p 453, 1987.

3. M. Saffman, "Optical Particle Sizing Using the Phase of LDA Signal.", Dantec Information No. 5, Sept. 1987.

4. S. A. M. Al-Chalabi, Y. Hardalupas, A. R. Jones, and A. M. K. P. Taylor, "Calculation of Calibration Curves for the Phase Doppler Technique: Comparison Between Mie Theory and Geometrical Optics.", International Symposium on Optical Paricle Sizing: Theory and Practice, Mont Saint-Aignan, France

5. W. D. Bachalo and S. V. Sankar, "Analysis of the Light Scattering Interferometery for Spheres Larger Than the Light Wavelength.", Fourth International Symposium on Applications Laser Anemometry to Fluid Mechanics, Lisbon, Portugal, July, 1988.

6. J. D. Pendleton, "A Generalized Mie Theory Solution and Its Application to Particle Sizing Interferometery.", Ph.D Thesis, University of Tennessee, Knoxville, June, 1982.

7. W. P. Chu and D. M. Robinson, "Scattering from a moving Spherical Particle by Two Crossed Coherent Plane Waves.", Applied Optics Vol. 16, p 619, 1977.

8. M. J. Rudd, "A self Aligning Laser Doppler Velocimeter.", Optical Instruments and Techniques, p158, 1969.